Centrin2 regulates CP110 removal in primary cilium formation

Suzanna L. Prosser and Ciaran G. Morrison

Centre for Chromosome Biology, School of Natural Sciences, National University of Ireland, Galway, Galway, Ireland

Primary cilia are antenna-like sensory microtubule structures that extend from basal bodies, plasma membrane–docked mother centrioles. Cellular quiescence potentiates ciliogenesis, but the regulation of basal body formation is not fully understood. We used reverse genetics to test the role of the small calcium-binding protein, centrin2, in ciliogenesis. Primary cilia arise in most cell types but have not been described in lymphocytes. We show here that serum starvation of transformed, cultured B and T cells caused primary ciliogenesis. Efficient ciliogenesis in chicken DT40 B lymphocytes required centrin2. We disrupted *CETN2* in human retinal pigmented epithelial cells, and despite having intact centrioles, they were unable to make cilia upon serum starvation, showing abnormal localization of distal appendage proteins and failing to remove the ciliation inhibitor CP110. Knockdown of *CP110* rescued ciliation in *CETN2*-deficient cells. Thus, centrin2 regulates primary ciliogenesis through controlling CP110 levels.

Introduction

Primary cilia are crucial for several signal transduction pathways (Goetz and Anderson, 2010). Their assembly is an ordered process that must be closely integrated with the cell cycle because of the dual roles of centrioles in ciliation and in mitosis (Sorokin, 1962; Seeley and Nachury, 2010; Ishikawa and Marshall, 2011). After cell division, a daughter cell inherits a centrosome that consists of pericentriolar material (PCM) in which are embedded two centrioles, barrel-shaped structures of triplet microtubules arranged with a ninefold symmetry. The centrioles differ from one another: the older of the two carries distal and subdistal appendages and is termed the mother centriole, as distinct from the younger, daughter centriole. During centrosome duplication in S phase, both centrioles will serve as the foundation for new procentrioles, although the daughter only acquires its appendages later in the cycle (Nigg and Stearns, 2011). These appendages are key to the plasma membrane recruitment of the mother centriole to serve as a basal body, the structure from which the ciliary axoneme extends in a membrane-bounded, nine-membered array of doublet microtubules.

Primary cilia are found in most cell types in the body but have not been described in lymphocytes. Although the reasons for a general lack of ciliation in lymphocytes are unclear, it is possible that this is related to the requirement of centrosomes for immune cell function. The movement of centrosomes toward the immune synapse, a membrane region at which cells of the immune system contact their target cells, helps to establish a specialized structure that has several similarities with cilia (Stinchcombe and Griffiths, 2014). Although no axoneme is formed at the immune synapse, several ciliary components have been implicated in immune synapse functions (Finetti et al., 2009), so that certain immune cell functions may not be compatible with the capacity for primary ciliogenesis (Griffiths et al., 2010). However, whether lymphocytes are capable of making cilia is an open question.

The mechanism that controls the functional change from centriole to basal body is not fully understood (Kobayashi and Dynlacht, 2011). A complex that includes CP110 and Cep97 acts as a cap at the distal end of centrioles to block mother centriole conversion to a basal body (Kleylein-Sohn et al., 2007; Spektor et al., 2007; Tsang et al., 2008). CP110 levels are regulated during the cell cycle by targeted degradation through the ubiquitin–proteasome system (D'Angiolella et al., 2010; Li et al., 2013), with TTBK2 (tau tubulin kinase 2) also being required for efficient removal of CP110 (Goetz et al., 2012; Čajánek and Nigg, 2014). Another interactor of CP110 is centrin2, a small, highly conserved calcium-binding protein, although the functional significance of this interaction in cilium regulation is unknown

Correspondence to Ciaran G. Morrison: Ciaran.Morrison@nuigalway.ie

Abbreviations used in this paper: hTERT, human telomerase reverse transcriptase; PCM, pericentriolar material; SAG, Smoothened agonist; TEM, transmission EM.

The Rockefeller University Press $30.00
J. Cell Biol. Vol. 208 No. 6 693–701
www.jcb.org/cgi/doi/10.1083/jcb.201411070

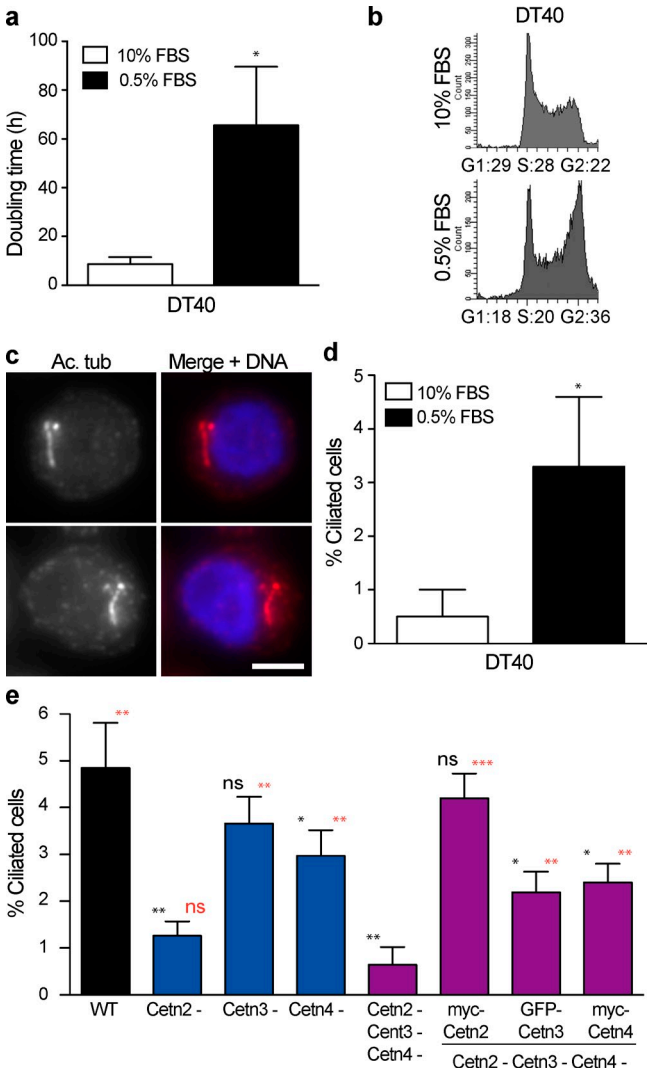

Figure 1. **Centrin2 is required for ciliation in chicken B-cells.** (a and b) Quantitation of doubling time (a) and flow cytometry analysis of DNA content (b) in DT40 cells after 48-h culture in 10% normal medium or serum starvation in 0.5% FBS. Bar graph shows means + SD of three independent experiments. *, $P < 0.05$, compared with controls by unpaired *t* test. Numbers under FACS plots indicate mean percentages of the entire population in the indicated cell cycle stage ($n = 4$). (c) Immunofluorescence microscopy of the cilium marker, acetylated tubulin, in serum-starved DT40 cells. Ac. tub, acetylated tubulin. Bar, 5 µm. (d) Quantitation of the number of cells with acetylated tubulin staining in DT40 cells cultured for 48 h in the indicated medium. Histogram shows means + SD of three independent experiments in which ≥500 cells were quantitated. *, $P < 0.05$, compared with controls by unpaired *t* test. (e) Quantitation of the number of cells with acetylated tubulin staining in wild-type (WT) and the indicated centrin-deficient and rescued DT40 clones after 48-h serum starvation. Histogram shows means + SD of three independent experiments in which at least 500 cells were quantitated. *, $P < 0.05$; **, $P < 0.01$; ***, $P < 0.001$, by unpaired *t* test. Black asterisks, comparison to WT cells; red asterisks, comparison to triple *Cetn4*$^{-/-}$ *Cetn2*$^{-/-}$ *Cetn3*$^{-}$ knockout cells.

(Tsang et al., 2006). Although centrin plays a critical role in centriole dynamics and ciliogenesis in lower eukaryotes, its roles in vertebrate cells are less clear (Dantas et al., 2012). Here, we explore the roles of centrin2 in ciliogenesis using a series of chicken lymphocytes with targeted mutations in all the centrin genes (Dantas et al., 2011) as well as gene disruption in the ciliated RPE1 cell line.

Results and discussion

Exit from the cell cycle into quiescence has long been established as potentiating ciliogenesis (Dingemans, 1969; Seeley and Nachury, 2010). We tested whether the chicken DT40 lymphocyte cell line could be induced to undergo primary ciliation. Serum starvation of chicken B-lymphocyte DT40 cells led to cell cycle delay (Fig. 1, a and b) and a reproducible induction of primary cilia (Fig. 1, c and d). The ability to induce cilia in DT40 cells allowed us to explore the roles of centrin in ciliogenesis. Examining a series of genetically defined centrin knockout lines (Dantas et al., 2011), we found that centrin2 deficiency led to a significant decline in ciliation capacity that was as extensive as the decline seen in cells that lacked all three chicken centrin isoforms. Although the expression of centrin3 and centrin4 could partially rescue the absence of all chicken centrins in ciliogenesis, only the expression of centrin2 led to a complete rescue of the ability of DT40 cells to make primary cilia after serum starvation (Fig. 1 e), demonstrating that centrin2 is required for ciliation in lymphocytes. Centrin2 depletion in zebrafish gave rise to several ciliopathy phenotypes (Delaval et al., 2011) and a mouse knockout also revealed marked ciliopathy that was restricted to specific tissues (Ying et al., 2014). It was concluded that the murine phenotype in affected tissues was caused by problems in ciliary trafficking, with normal ciliogenesis initiation and axoneme formation (Ying et al., 2014). Given the partial rescue of ciliation that we see with centrin3 and centrin4 in the chicken model, it is possible that the interplay between the individual members of the centrin family determines the precise roles of an individual centrin in a given tissue.

As ciliogenesis has not been described in lymphocytes before, to our knowledge, we wished to confirm that we were observing bona fide cilia. We used serum starvation to induce ciliogenesis in human Jurkat T-lymphocytes and NALM-6 B cells. Culturing these lines in 0.5% serum, instead of the standard 10%, caused marked increases in their doubling times and cell cycle delays (Fig. 2, a and b). When we stained serum-starved Jurkat or NALM-6 cells with antibodies to acetylated tubulin, we reproducibly observed linear structures that resembled primary cilia (Fig. 2, c and d). The base of these structures contained centrioles, as determined by Cep135 and centrin3 staining, within apparently normal PCM, as visualized by pericentrin and γ-tubulin (Fig. 2 e). In addition, the established cilia markers IFT88, Arl13B, PDGFR-α, Gli2, Patched, and detyrosinated tubulin all localized to these structures (Fig. 2, f and g) and treatment of serum-starved NALM-6 cells with Smoothened agonist (SAG) led to the localization of Smoothened (Fig. 2 h), indicative of their functioning as cilia. Depletion of the negative ciliary regulator CP110 by siRNA treatment also induced these structures (Fig. 2, i and j), suggesting that their regulation is similar to that of primary cilia (Spektor et al., 2007). The structures induced by CP110 knockdown in lymphocytes did not contain centrin3, which was restricted to the basal body (Fig. 2 k), and were positive for the ciliary markers Arl13B and PDGFR-α (Fig. 2 l). Transmission EM (TEM) revealed the membrane association of the mother centriole, the nucleation

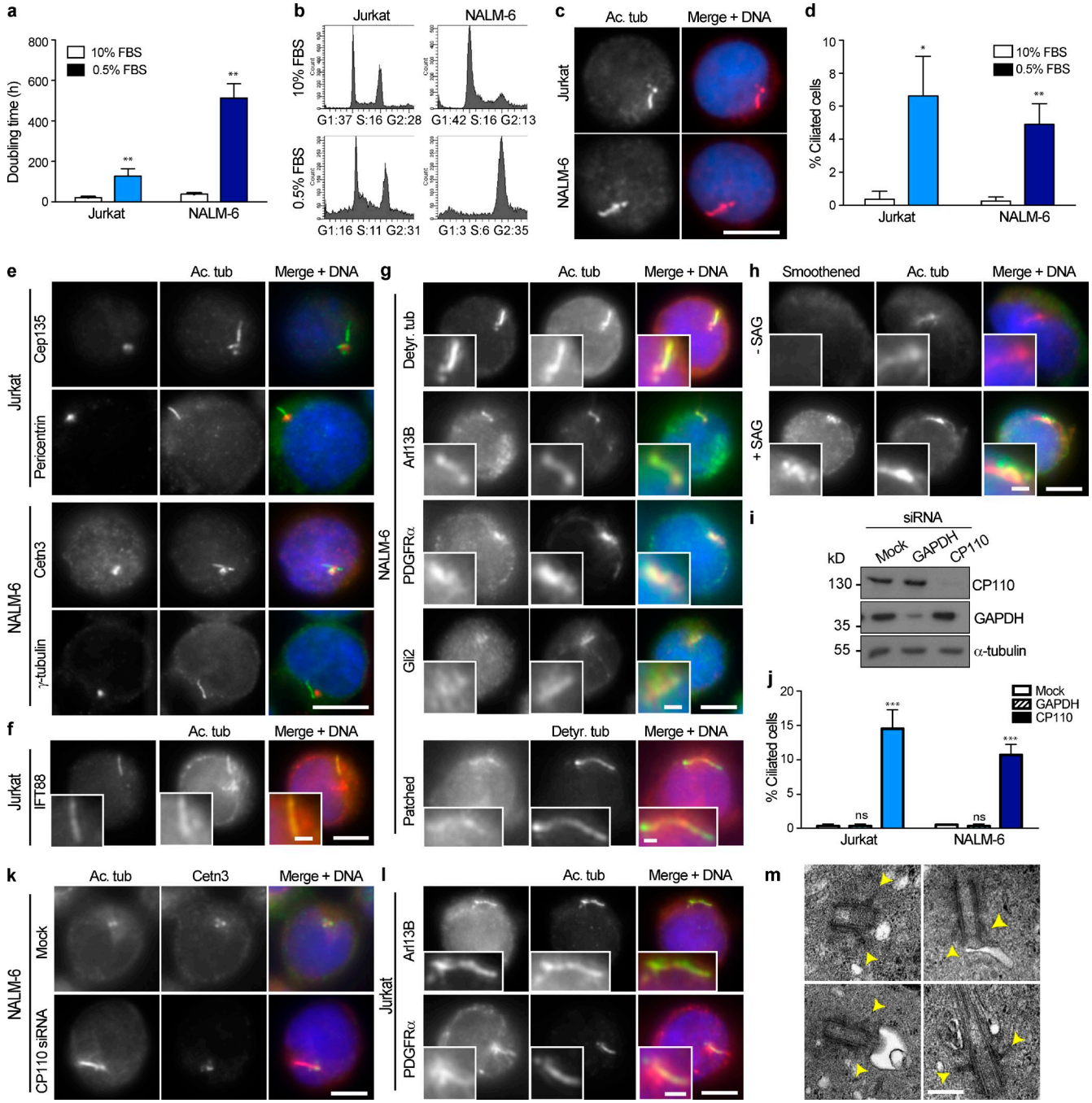

Figure 2. **Serum starvation and CP110 depletion both lead to ciliation in human lymphocytes.** (a and b) Quantitation of doubling time (a) and flow cytometry analysis of DNA content (b) in Jurkat and NALM-6 cells. Bar graph shows means + SD of three independent experiments. **, $P < 0.01$, compared with controls by unpaired *t* test. Numbers under FACS plots indicate mean percentages of the entire population in the indicated cell cycle stage ($n = 3$ for Jurkat cells and 2 for NALM-6 cells). Jurkat cells were serum starved in 0.5% FBS for 72 h and NALM-6 for 100 h. (c) Immunofluorescence microscopy of the cilium marker acetylated tubulin in serum-starved Jurkat and NALM-6 cells. (d) Quantitation of the number of cells with acetylated tubulin (Ac. tub) staining in Jurkat and NALM-6 cells grown in media containing 10% or 0.5% FBS. Histogram shows means + SD of three independent experiments in which ≥500 cells were quantitated. *, $P < 0.05$; **, $P < 0.01$, compared with controls of the same cell line by unpaired *t* test. (e) Immunofluorescence microscopy of the indicated PCM and centriolar markers in serum-starved Jurkat and NALM-6 cells. Cetn3, centrin3. (f) Immunofluorescence microscopy of IFT88 alongside acetylated tubulin in serum-starved Jurkat cells. (g) Immunofluorescence microscopy of the indicated cilium markers in serum-starved NALM-6 cells. Detyr. tub, detyrosinated tubulin. (h) Immunofluorescence microscopy of Smoothened in the absence and presence of SAG in serum-starved NALM-6 cells. (i) Immunoblot showing depletion of CP110 and GAPDH by siRNA in NALM-6 cells. (j) Quantitation of the number of cells with acetylated tubulin staining in mock-treated, GAPDH, and CP110-depleted Jurkat and NALM-6 cells. Histogram shows means + SD of three independent experiments in which ≥500 cells were quantitated. ***, $P < 0.001$, compared with mock-treated cells of the same cell line by unpaired *t* test. (k) Immunofluorescence microscopy of acetylated tubulin and centrin3 in mock and CP110-depleted NALM-6 cells. (l) Immunofluorescence microscopy of the cilium markers Arl13B and PDGFR-α in CP110-depleted Jurkat cells. (m) TEM micrographs of centrioles and associated structures from NALM-6 cells depleted of CP110 for 100 h. Subdistal appendages are indicated by yellow arrowheads. Insets show enlarged images of cilia. Bars: (c, e, f–h [main images], k, and l [main images]) 5 µm; (f–h and l [insets]) 1 µm; (m) 200 nm.

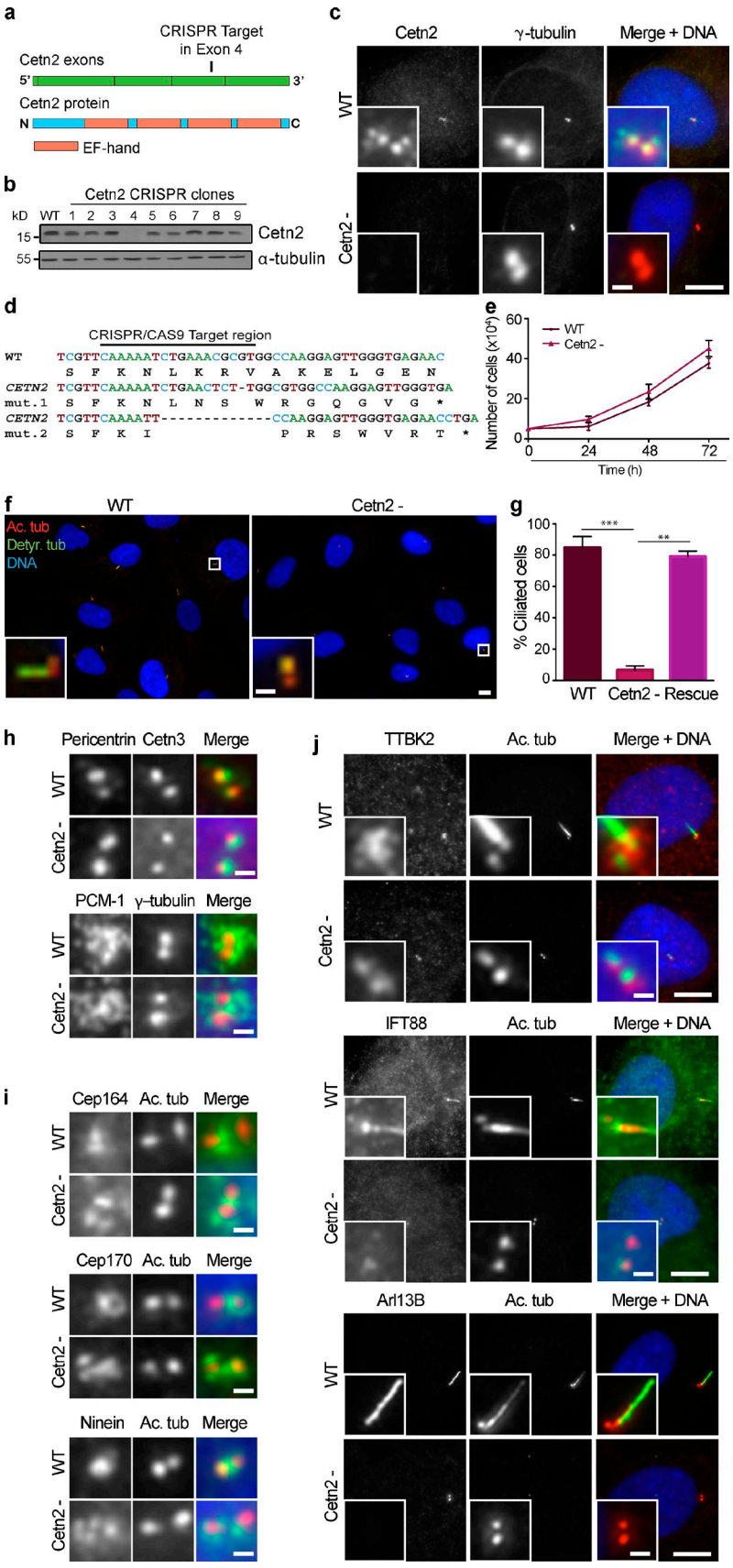

Figure 3. **Centrin2 is required for primary cilium formation in human epithelial cells.** (a) Schematic showing the targeted region in exon 4 of the *CETN2* gene and corresponding location in the third EF-hand of the centrin2 protein. (b and c) Loss of centrin2 protein expression was confirmed by immunoblot and immunofluorescence microscopy. Insets show enlarged images of centrioles. (d) Sequence analysis revealed the presence of indels that lead to premature stop codons. mut., mutation. (e) Growth curve of wild-type (WT) and centrin2-null hTERT-RPE1 cells. Data points show means ± SD of three independent experiments. No significant difference was observed between wild-type and centrin-deficient cells at any time point. (f) Immunofluorescence microscopy of the cilium markers acetylated and detyrosinated tubulin in wild-type and centrin2-null cells after 48-h serum starvation. Insets show enlarged images of centrioles/basal bodies. Ac. tub, acetylated tubulin; Detyr. tub, detyrosinated tubulin. (g) Quantitation of the ciliation frequency after 48-h serum starvation in wild-type, centrin2-null cells, and centrin2-null cells transiently rescued with centrin2-GFP. Histogram shows means + SD of three independent experiments in which ≥200 cells were quantitated. **, $P < 0.01$; ***, $P < 0.001$, in comparison to the indicated samples by unpaired *t* test. (h) Immunofluorescence microscopy of the indicated PCM, centriole, and centriolar satellite makers in asynchronous wild-type and centrin2-null cells. (i) Immunofluorescence microscopy of the indicated appendage markers in asynchronous wild-type and centrin2-null cells. (j) Immunofluorescence microscopy of the indicated proteins in serum-starved wild-type and centrin2-null hTERT-RPE1 cells. Insets show enlarged images of centrioles/basal bodies. Bars: (c, f, and j [main images]) 10 µm; (c and f [insets], h, i, and j [insets]) 1 µm.

of vesicles that resemble the ciliary pocket, and the extension of axoneme-like structures in CP110-depleted lymphocytes (Fig. 2 m). Along with the immunofluorescence microscopy of cilium-specific markers, the TEM data provide strong support for these being primary cilia, rather than the extended centrioles that have been described in nonciliating U2OS cells

upon CP110 knockdown (Kohlmaier et al., 2009; Schmidt et al., 2009; Tang et al., 2009). Together, these data indicate that apparently normal, functional primary cilia can be induced in cultured lymphocytes, albeit with the obvious caveats that these are transformed cell lines and that the efficiency of this process is low. Although significant lymphocyte populations are quiescent for long periods and thus might be expected to use ciliation as a regulatory mechanism, whether lymphocytes make cilia in the body remains to be determined, especially given the additional roles required of the centrosomes in immune cell functioning (Stinchcombe and Griffiths, 2014).

To address the question of how centrin2 contributes to ciliogenesis in cells that normally form cilia, we used the CRISPR (clustered regularly interspaced short palindromic repeat)-Cas9 system of RNA-guided endonuclease activity to disrupt the sequence coding for centrin2 in the immortalized, nontransformed human telomerase reverse transcriptase (hTERT)–RPE1 cell line (Jinek et al., 2012). The guide RNAs were designed to target exon 4 of *CETN2*, which encodes the third of centrin's four calcium-binding EF-hands (Fig. 3 a). Immunoblot and immunofluorescence microscopy screening identified a centrin-deficient clone (Fig. 3, b and c), and DNA sequence analysis confirmed two mutations that led to premature stop codons in the centrin2 coding sequence (Fig. 3 d). This null clone was used for our analysis (Fig. 3 b, clone 4). Centrin2-deficient cells showed no proliferation defect, even proliferating more rapidly than wild-type controls (Fig. 3 e). Wild-type RPE1 cells underwent high levels of ciliogenesis upon serum starvation, with >80% of cells carrying primary cilia, but <10% of centrin2-deficient cells made cilia under the same circumstances (Fig. 3, f and g). Previous work in hTERT-RPE1 cells using siRNA to deplete centrin2 also observed declines in ciliation capacity, albeit only to ∼40% of control levels, which may reflect technical differences between the analysis of null and knockdown cells (Graser et al., 2007; Mikule et al., 2007). Importantly, expression of centrin2 in our knockout cells restored their ciliation capacity to wild-type levels (Fig. 3 g).

Examining potential mechanisms for the ciliation defect in centrin2-deficient cells, we found that centrin2 ablation did not affect centriole or PCM integrity, as determined by microscopy of centrin3, pericentrin, and γ-tubulin (Fig. 3 h). PCM-1 staining indicated intact centriolar satellite formation in the absence of centrin2 (Fig. 3 i). However, we did observe marked alterations in the composition of the distal end of centrioles in centrin-deficient cells. As shown in Fig. 3 i, both centrioles carried Cep164, Cep170, and ninein, which are normally limited to the mother centriole, with a marked dispersion of the Cep164 and ninein signals away from their normal localization at the distal end of the centrioles (Ou et al., 2002; Graser et al., 2007). Although we observed centriolar localization of TTBK2 and IFT88, these were not incorporated into ciliary structures (Fig. 3 j). Furthermore, we did not observe any Arl13b at centrioles, confirming the absence of ciliary function in centrin2-deficient cells (Fig. 3 j). These observations suggested that the principal defect in centrin2 nulls lies at the distal end of the centriole and, thus, in the potential for converting centrioles to basal bodies.

TEM confirmed the integrity of the centrioles in centrin2-deficient cells (Fig. 4 a). This analysis also demonstrated that centrioles docked successfully with ciliary vesicles, a key early step in ciliogenesis that is directed by Cep164 (Fig. 4 a; Sorokin, 1962; Schmidt et al., 2012; Tanos et al., 2013). Despite the abnormal Cep164 distribution that we saw in centrin-deficient cells, this observation indicates that the distal appendages are capable of allowing docking and that the defect in ciliation lies at a later stage in the process.

After docking, the extension of the centriole into the vesicle forms the ciliary axoneme (Sorokin, 1962; Schmidt et al., 2012). Centrin2-deficient cells did not carry out this step. A crucial requirement for axoneme outgrowth is the removal of CP110 and its partner protein, Cep97, from the distal end of the mother centriole (Spektor et al., 2007; Tsang et al., 2008). CP110 was present at both centrioles in cycling wild-type and centrin2-deficient cells and was then lost from the wild-type mother centriole upon cilium induction by serum starvation (Fig. 4 b). Notably, this removal of CP110 did not occur in centrin2-null cells, with cells instead acquiring multiple foci of CP110 around the centrioles (Fig. 4 b). Similarly, Cep97 was not removed from the mother centriole, but, in fact, its signal increased around the centrioles (Fig. 4 c). The CP110 signals now colocalized with centriolar satellites (Fig. 4 d), suggesting a marked alteration of CP110 dynamics in the absence of centrin2. Although serum starvation of wild-type cells led to a decline in cellular levels of CP110 and Cep97, centrin2-deficient cells maintained high levels of both proteins (Fig. 4 e). Interestingly, serum starvation induced a notable increase in centrin2 levels. An increase in p16 levels was seen in response to serum starvation in both wild-type and centrin2-deficient cells, indicating that centrin2 loss did not blunt general cellular responses to nutrient deprivation (Fig. 4 e). Although recent work has indicated that autophagy regulates primary cilium formation (Pampliega et al., 2013; Tang et al., 2013), we found no effect of centrin2 deficiency on cellular levels of the autophagy-regulating E3 ligase, Atg5, or the autophagy substrate, LC3B, suggesting this is not the primary mechanism by which centrin2 regulates ciliation (Fig. 4 e). We next tested whether the ciliary defect in centrin2 knockout cells could be attributed solely to CP110 dysregulation by depleting CP110 using siRNA. As shown in Fig. 4 (f–h), CP110 knockdown rescued primary ciliation in serum-starved centrin2-deficient cells, demonstrating that CP110 removal is the key activity mediated by centrin2 in allowing ciliation.

One mechanism that regulates CP110 removal acts through TTBK2 at basal bodies, although the relevant targets of this kinase are not yet defined (Goetz et al., 2012; Čajánek and Nigg, 2014). While TTBK2 localized to centrin2-deficient centrioles, its asymmetric recruitment to the mother centriole was lost (Fig. 3 j). One way centrin2 might regulate CP110 may be through the localization of TTBK2 and Cep164, given the reported interactions of these proteins (Čajánek and Nigg, 2014). Another mechanism that removes CP110 involves its ubiquitination and subsequent degradation through the ubiquitin ligase complex $SCF^{cyclin\ F}$ (D'Angiolella et al., 2010), an activity that is opposed by the deubiquitinating enzyme USP33 (Li et al., 2013). We found that serum starvation led to a marked reduction in

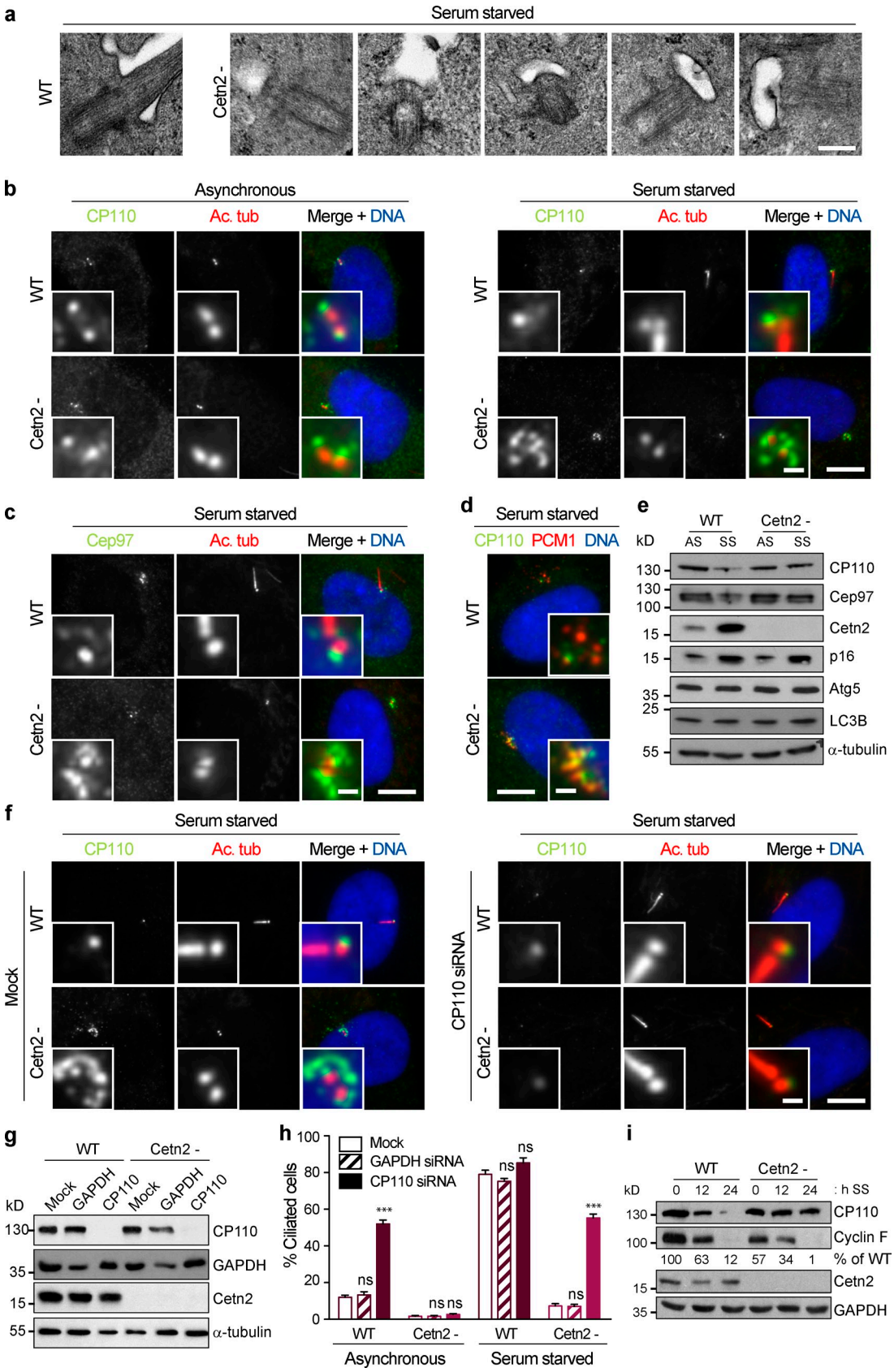

Figure 4. **Centrin2 is required for the removal of CP110 and Cep97 from centrioles upon serum starvation.** (a) TEM analysis of wild-type (WT) and centrin2-null cells after 48-h serum starvation. (b) Immunofluorescence microcopy of CP110 and acetylated tubulin (Ac. tub) in asynchronous or 48-h serum-starved wild-type and centrin2-null cells. Insets in b–f show enlarged images of centrioles/basal bodies. (c) Immunofluorescence microscopy of Cep97 and acetylated tubulin in 48-h serum-starved wild-type and centrin2-null cells. (d) Immunofluorescence microscopy of CP110 and PCM1 in serum-starved wild-type and

cyclin F levels in both wild-type and centrin2-deficient cells but that there was a greater decline in cyclin F levels in centrin2-null cells (Fig. 4 i), suggesting another possibility for how centrin deficiency may impede the removal of CP110 from centrioles. Therefore, the regulation of TTBK2 localization or activity, as well as the control of cyclin F activity at the distal end of the centriole, both remain as potential mechanisms by which centrin2 directs CP110 removal to permit ciliogenesis.

Materials and methods

Cells and cell culture

All human cell lines were maintained in a humidified 5% CO_2 atmosphere at 37°C. Jurkat E6.1 human T cells were obtained from Sigma-Aldrich; NALM-6 human B cells were obtained from the Leibniz Institute-German Collection of Microorganisms; and hTERT-RPE1 cells were obtained from ATCC. Jurkat and NALM-6 cells were grown in RPMI 1640 (Gibco) supplemented with 10% vol/vol FBS (Sigma-Aldrich) and penicillin-streptomycin (100 U/ml and 100 µg/ml, respectively; Sigma-Aldrich). hTERT-RPE1 cells were grown in DMEM/F12 1:1 (Lonza) supplemented with 10% FBS and penicillin-streptomycin. Chicken DT40 B cells were maintained in a humidified 5% CO_2 atmosphere at 39.5°C. The DT40 single *Cetn2*$^{-/-}$, *Cetn3*$^{-}$, and *Cetn4*$^{-/-}$ and triple *Cetn4*$^{-/-}$ *Cetn2*$^{-/-}$ *Cetn3*$^{-}$ knockouts were generated using gene targeting (Dantas et al., 2011, 2013). Stable transfection into the triple *Cetn4*$^{-/-}$ *Cetn2*$^{-/-}$ *Cetn3*$^{-}$ knockouts of plasmids that expressed myc-Cetn2, GFP-Cetn3, and myc-Cetn4 under the control of the cytomegalovirus promoter in pCMV-3tag or pEGFP-C1 gave the centrin rescue cell lines previously described (Dantas et al., 2011). DT40 cells were grown in RPMI 1640 supplemented with 10% FBS, 1% vol/vol chicken serum (Sigma-Aldrich), and penicillin-streptomycin. For serum starvation experiments, Jurkat cells were plated at 0.2 × 10^6 cells/ml in RPMI 1640 media supplemented with 0.5% FBS for 72 h; NALM-6 cells were plated at 0.75 × 10^6 cells/ml in RPMI 1640 media supplemented with 0.5% FBS for 100 h; and DT40 cells were plated at 0.15 × 10^6 cells/ml in RPMI 1640 media supplemented with 0.5% FBS and 1% chicken serum for 48 h. Primary cilia formation was induced in hTERT-RPE1 cells by culturing cells in DMEM/F12 supplemented with 0.1% FBS for up to 48 h. To deplete cells of serum, cells were washed twice with PBS followed by two washes with reduced serum media before being plated in fresh reduced serum media for the duration of the experiment. The SAG (CAS 364590–63-6; EMD Millipore) was used at 100 nM for 4 h to induce movement of Smoothened into the primary cilium.

CRISPR/Cas9 targeting of *CETN2* in hTERT-RPE1 cells

RNA-guided targeting of *CETN2* in hTERT-RPE1 cells was achieved through coexpression of the Cas9 protein with guide RNAs. A guide RNA expression plasmid was generated by inserting annealed primers into the pX333-U6-Chimeric_BB-CBh-hSpCas9 vector (plasmid 43330; Addgene; deposited by F. Zhang, Massachusetts Institute of Technology, Cambridge, MA; Cong et al., 2013) digested by BbsI. Primers targeting exon 4 were designed based on the human exome Cas9 site catalogs (Mali et al., 2013): forward primer 5′-CACCGGTTCAAAAATCTGAAACGCG-3′ and reverse primer 5′-AAACCGCGTTTCAGATTTTTGAACC-3′. For transfection, 3 µg plasmid DNA was complexed with Lipofectamine 2000 (Invitrogen) in serum-free OptiMEM (Gibco) according to the manufacturer's instructions and added to cells at 70% confluency. The following day, the transfected cells were serially diluted, and individual colonies were picked and expanded 10 d later. Screening of CETN2 protein levels by Western blotting and immunofluorescence microscopy was used to confirm loss of protein expression. Genomic DNA was extracted and subjected to PCR using a forward primer to intron 3, 5′-CCGCAAGTCTAGACTCGAG-3′, and reverse primer to intron 4, 5′-CCTTGAAGATTGCCTTGACTAG-3′, to generate a product spanning the targeted region. The PCR product was cloned into pGEM-T-Easy (Promega), and DNA was prepared from individual bacterial colonies and sent for commercial sequencing.

RNA-mediated interference

Silencer Select siRNA oligonucleotides specific to *CP110* (#1 sense, 5′-GCAAAACCAGAAUACGAGATT-3′, and antisense, 5′-UCUCGUAUUCUGGUUUUGCAT-3′; and #2 sense, 5′-CAAGCGGACUCACUCCAUATT-3′, and antisense, 5′-UAUGGAGUGAGUCCGCUUGAG-3′) or *GAPDH* as an experimental control (sense, 5′-UGGUUUACAUGUUCCAAUATT-3′, and antisense, 5′-UAUUGGAACAUGUAAACCATG-3′) were purchased from Ambion. For suspension cells, 50 nmol siRNA was transfected using Amaxa Nucleofector Kit V (Jurkat) or Kit T (NALM-6) according to the manufacturer's instructions (Lonza). Cells were analyzed by Western blotting and immunofluorescence microscopy 72 h (Jurkat) or 100 h (NALM-6) after transfection. For hTERT-RPE1 cells, 50 nmol siRNA was complexed with Oligofectamine (Invitrogen) in serum-free OptiMEM (Gibco) according to the manufacturer's instructions. 24 h after transfection, cells were serum starved as described for 24 h before analysis by Western blotting and immunofluorescence microscopy.

Transient transfection

For transient rescue experiments pCETN2-GFP (Inanç et al., 2010) was transfected into CETN2-null hTERT-RPE1 cells. 1 µg plasmid DNA was complexed with Lipofectamine 2000 in serum-free OptiMEM and added to cells at 60% confluency. 24 h after transfection, cells were serum starved as described for 24 h before analysis by immunofluorescence microscopy.

Immunofluorescence microscopy

Adherent cells (hTERT-RPE1) were grown on glass coverslips while suspension cells (Jurkat, NALM-6, and DT40) were attached to poly-L-lysine–coated slides for 10 min at 4°C. Cells were fixed in methanol/5 mM EGTA at −20°C for 10 min or 4% paraformaldehyde for 7 min at room temperature followed by permeabilization with 0.15% Triton X-100 in PBS for 30 s. Before fixation and staining with acetylated tubulin, cells were incubated on ice for 30 min to depolymerize microtubules. The cells were blocked in 1% BSA in PBS and incubated with primary antibodies for 1 h at room temperature followed by a 45-min incubation with secondary antibodies. Donkey secondary antibodies were labeled with Alexa Fluor 488, Alexa Fluor 594, or Rhodamine (Jackson ImmunoResearch Laboratories, Inc.). DNA was stained with Hoechst 33258 (Sigma-Aldrich). Slides were mounted with 3% wt/vol *N*-propyl-gallate and 80% vol/vol glycerol in PBS. Images were captured with a camera (Orca AG; Hamamatsu Photonics) under oil at room temperature on a microscope (IX71; Olympus), 100× oil objective, NA 1.35, using Volocity software (PerkinElmer), and merges and individual channel images were exported as TIFFs for publication. Images were then cropped for publication using Photoshop CS6 (Adobe). Mouse monoclonal antibodies used were as follows: acetylated tubulin (1:2,000; T6793; Sigma-Aldrich), γ-tubulin (1:1,000; T6557; Sigma-Aldrich), and Centrin3 (1:1,000; 3E6; Abnova). Rabbit polyclonal antibodies used were against γ-tubulin (1:1,000; T3559; Sigma-Aldrich), Cep135 (1:1,000; ab75005; Abcam), Pericentrin (1:1,000; ab4448; Abcam), Centrin2 (1:500; 6288; BioLegends), Ninein (1:200; ab4447; Abcam), Cep164 (1:250; NBP1-77006; Novus Biologicals), Cep170 (1:1,000; raised against His-tagged amino acids 15–754 of human Cep170, a gift from G. Guarguaglini, University of Rome, Rome, Italy; Guarguaglini et al., 2005), PCM-1 (1:1,000; raised against His-tagged amino acids 1,665–2,024 of the human PCM-1, a gift from A. Merdes, University of Toulouse, Toulouse, France; Dammermann and Merdes, 2002), CP110 (1:500; 12780–1-AP; Proteintech), Arl13b (1:500; 17711–1-AP; Proteintech), IFT88 (1:800; 13967–1-AP; Proteintech), Gli2 (1:200; sc-28674; Santa Cruz Biotechnology, Inc.), PDGFR-α (1:200; sc-338; Santa Cruz Biotechnology, Inc.), detyrosinated tubulin (1:800; ab48389; Abcam), and Smoothened (1:500;

centrin2-null cells. (e) Immunoblot analysis of the indicated proteins in asynchronous (AS) and 48-h serum-starved (SS) wild-type and centrin2-null cells. (f) Immunofluorescence microscopy of CP110 and acetylated tubulin in mock-treated or CP110-depleted cells. (g) Immunoblot analysis of the indicated proteins in mock, GAPDH, and CP110-depleted WT and centrin2-null cells after 24-h serum starvation after transfection. (h) Frequency of ciliated cells in mock, GAPDH, and CP110-depleted wild-type and centrin2-null cells either grown asynchronously or serum starved for 24-h after transfection. Histogram shows means + SD of three independent experiments in which ≥200 cells were quantitated. ***, $P < 0.001$, in comparison to mock-treated control cells by unpaired *t* test. (i) Immunoblot analysis of the indicated proteins in wild-type and centrin2-null cells after serum starvation for the indicated period. Numbers indicate the mean cyclin F band intensity per lane expressed as a percentage of the signal in wild type at 0 h ($n = 3$). Bars: (a) 200 nm; (b, c, and f [main images]) 10 µm; (b, c, and f [insets]) 1 µm.

ab38686; Abcam). Goat polyclonal antibodies used were against PCM-1 (1:1,000, for costaining with CP110; sc-50164; Santa Cruz Biotechnology, Inc.), Patched (1:200; sc-6149; Santa Cruz Biotechnology, Inc.), and TTBK2 (1:500; sc-165430; Santa Cruz Biotechnology, Inc.).

Immunoblotting

Whole-cell extracts were prepared with radioimmunoprecipitation assay buffer (50 mM Tris-HCl, pH 7.4, 1% NP-40, 0.25% sodium deoxycholate, 150 mM NaCl, and 1 mM EDTA, with protease and phosphatase inhibitor cocktails). Extracts were boiled in loading buffer for 5 min. Proteins were separated on 10 or 15% SDS-PAGE gels and transferred to nitrocellulose membranes (GE Healthcare) for analysis. Blots were detected by ECL (GE Healthcare). Primary antibodies used were rabbit polyclonals against Atg5 (1:500; NB110-53818; Novus Biologicals), Centrin2 (1:1,000; 6288; Bio-Legends), CP110 (1:2,000; 12780–1-AP; Proteintech), Cep97 (1:5,000; 22050–1-AP; Proteintech), Cyclin F (1:1,000; sc-952; Santa Cruz Biotechnology, Inc.), and LC3B (1:500; 2775; Cell Signaling Technology); rabbit monoclonal against GAPDH (1:10,000; 2118; Cell Signaling Technology); and mouse monoclonals against α-tubulin (1:10,000; T5168; Sigma-Aldrich), and p16 (1:1,000; sc-56330; Santa Cruz Biotechnology, Inc.). HRP-conjugated goat anti–mouse or anti–rabbit secondary antibodies were used at 1:5,000 (Jackson ImmunoResearch Laboratories, Inc.). Band quantitation was performed using ImageJ version 1.48 (National Institutes of Health).

Flow cytometry

For flow cytometry, cells were fixed with ice-cold 70% ethanol at −20°C overnight. After fixation, cells were washed twice with PBS then resuspended in PBS containing 200 µg/ml RNase A and 40 µg/ml propidium iodide. Cytometry was performed on a FACSCanto (BD).

TEM

Cells were pelleted at 250 *g* for 5 min, washed twice with PBS, and then twice with 0.1 M sodium cacodylate buffer, pH 7.2 (Sigma-Aldrich), before primary fixation in 2% glutaraldehyde and 2% paraformaldehyde (Electron Microscopy Sciences) in cacodylate buffer overnight at 4°C. Cells were then secondarily fixed in 2% osmium tetroxide (Sigma-Aldrich) in cacodylate buffer for 2 h at room temperature. The cell pellet was then dehydrated through an ethanol gradient (30, 60, 90, and 100%) followed by propylene oxide. Subsequently, cells were embedded in Low Viscosity Resin (TAAB). Sections were cut on a microtome (Reichert-Jung Ultracut E; Leica), stained with uranyl acetate and lead citrate, and then viewed on a transmission electron microscope (H-7000; Hitachi). Images were taken with a camera (ORCA-HRL; Hamamatsu Photonics) and processed using AMT version 6 (AMT Imaging).

We thank Pierce Lalor at the National Biophotonics and Imaging Platform Ireland for technical assistance with the TEM, Tiago Dantas for cell lines, and Elaine Dunleavy for comments on the manuscript.

A Higher Education Authority PRTLI4 grant supported the National Biophotonics and Imaging Platform Ireland. This work was funded by the Science Foundation Ireland Principal Investigator award 10/IN.1/B2972.

The authors declare no competing financial interests.

Submitted: 17 November 2014
Accepted: 29 January 2015

References

Čajánek, L., and E.A. Nigg. 2014. Cep164 triggers ciliogenesis by recruiting Tau tubulin kinase 2 to the mother centriole. *Proc. Natl. Acad. Sci. USA*. 111:E2841–E2850. http://dx.doi.org/10.1073/pnas.1401777111

Cong, L., F.A. Ran, D. Cox, S. Lin, R. Barretto, N. Habib, P.D. Hsu, X. Wu, W. Jiang, L.A. Marraffini, and F. Zhang. 2013. Multiplex genome engineering using CRISPR/Cas systems. *Science*. 339:819–823. http://dx.doi.org/10.1126/science.1231143

Dammermann, A., and A. Merdes. 2002. Assembly of centrosomal proteins and microtubule organization depends on PCM-1. *J. Cell Biol.* 159:255–266. http://dx.doi.org/10.1083/jcb.200204023

D'Angiolella, V., V. Donato, S. Vijayakumar, A. Saraf, L. Florens, M.P. Washburn, B. Dynlacht, and M. Pagano. 2010. SCF(Cyclin F) controls centrosome homeostasis and mitotic fidelity through CP110 degradation. *Nature*. 466:138–142. http://dx.doi.org/10.1038/nature09140

Dantas, T.J., Y. Wang, P. Lalor, P. Dockery, and C.G. Morrison. 2011. Defective nucleotide excision repair with normal centrosome structures and functions in the absence of all vertebrate centrins. *J. Cell Biol.* 193:307–318. http://dx.doi.org/10.1083/jcb.201012093

Dantas, T.J., O.M. Daly, and C.G. Morrison. 2012. Such small hands: the roles of centrins/caltractins in the centriole and in genome maintenance. *Cell. Mol. Life Sci.* 69:2979–2997. http://dx.doi.org/10.1007/s00018-012-0961-1

Dantas, T.J., O.M. Daly, P.C. Conroy, M. Tomas, Y. Wang, P. Lalor, P. Dockery, E. Ferrando-May, and C.G. Morrison. 2013. Calcium-binding capacity of centrin2 is required for linear POC5 assembly but not for nucleotide excision repair. *PLoS ONE*. 8:e68487. http://dx.doi.org/10.1371/journal.pone.0068487

Delaval, B., L. Covassin, N.D. Lawson, and S. Doxsey. 2011. Centrin depletion causes cyst formation and other ciliopathy-related phenotypes in zebrafish. *Cell Cycle*. 10:3964–3972. http://dx.doi.org/10.4161/cc.10.22.18150

Dingemans, K.P. 1969. The relation between cilia and mitoses in the mouse adenohypophysis. *J. Cell Biol.* 43:361–367. http://dx.doi.org/10.1083/jcb.43.2.361

Finetti, F., S.R. Paccani, M.G. Riparbelli, E. Giacomello, G. Perinetti, G.J. Pazour, J.L. Rosenbaum, and C.T. Baldari. 2009. Intraflagellar transport is required for polarized recycling of the TCR/CD3 complex to the immune synapse. *Nat. Cell Biol.* 11:1332–1339. http://dx.doi.org/10.1038/ncb1977

Goetz, S.C., and K.V. Anderson. 2010. The primary cilium: a signalling centre during vertebrate development. *Nat. Rev. Genet.* 11:331–344. http://dx.doi.org/10.1038/nrg2774

Goetz, S.C., K.F. Liem Jr., and K.V. Anderson. 2012. The spinocerebellar ataxia-associated gene Tau tubulin kinase 2 controls the initiation of ciliogenesis. *Cell*. 151:847–858. http://dx.doi.org/10.1016/j.cell.2012.10.010

Graser, S., Y.D. Stierhof, S.B. Lavoie, O.S. Gassner, S. Lamla, M. Le Clech, and E.A. Nigg. 2007. Cep164, a novel centriole appendage protein required for primary cilium formation. *J. Cell Biol.* 179:321–330. http://dx.doi.org/10.1083/jcb.200707181

Griffiths, G.M., A. Tsun, and J.C. Stinchcombe. 2010. The immunological synapse: a focal point for endocytosis and exocytosis. *J. Cell Biol.* 189:399–406. http://dx.doi.org/10.1083/jcb.201002027

Guarguaglini, G., P.I. Duncan, Y.D. Stierhof, T. Holmström, S. Duensing, and E.A. Nigg. 2005. The forkhead-associated domain protein Cep170 interacts with Polo-like kinase 1 and serves as a marker for mature centrioles. *Mol. Biol. Cell*. 16:1095–1107. http://dx.doi.org/10.1091/mbc.E04-10-0939

Inanç, B., H. Dodson, and C.G. Morrison. 2010. A centrosome-autonomous signal that involves centriole disengagement permits centrosome duplication in G2 phase after DNA damage. *Mol. Biol. Cell*. 21:3866–3877. http://dx.doi.org/10.1091/mbc.E10-02-0124

Ishikawa, H., and W.F. Marshall. 2011. Ciliogenesis: building the cell's antenna. *Nat. Rev. Mol. Cell Biol.* 12:222–234. http://dx.doi.org/10.1038/nrm3085

Jinek, M., K. Chylinski, I. Fonfara, M. Hauer, J.A. Doudna, and E. Charpentier. 2012. A programmable dual-RNA-guided DNA endonuclease in adaptive bacterial immunity. *Science*. 337:816–821. http://dx.doi.org/10.1126/science.1225829

Kleylein-Sohn, J., J. Westendorf, M. Le Clech, R. Habedanck, Y.D. Stierhof, and E.A. Nigg. 2007. Plk4-induced centriole biogenesis in human cells. *Dev. Cell*. 13:190–202. http://dx.doi.org/10.1016/j.devcel.2007.07.002

Kobayashi, T., and B.D. Dynlacht. 2011. Regulating the transition from centriole to basal body. *J. Cell Biol.* 193:435–444. http://dx.doi.org/10.1083/jcb.201101005

Kohlmaier, G., J. Loncarek, X. Meng, B.F. McEwen, M.M. Mogensen, A. Spektor, B.D. Dynlacht, A. Khodjakov, and P. Gönczy. 2009. Overly long centrioles and defective cell division upon excess of the SAS-4-related protein CPAP. *Curr. Biol.* 19:1012–1018. http://dx.doi.org/10.1016/j.cub.2009.05.018

Li, J., V. D'Angiolella, E.S. Seeley, S. Kim, T. Kobayashi, W. Fu, E.I. Campos, M. Pagano, and B.D. Dynlacht. 2013. USP33 regulates centrosome biogenesis via deubiquitination of the centriolar protein CP110. *Nature*. 495:255–259. http://dx.doi.org/10.1038/nature11941

Mali, P., L. Yang, K.M. Esvelt, J. Aach, M. Guell, J.E. DiCarlo, J.E. Norville, and G.M. Church. 2013. RNA-guided human genome engineering via Cas9. *Science*. 339:823–826. http://dx.doi.org/10.1126/science.1232033

Mikule, K., B. Delaval, P. Kaldis, A. Jurcyzk, P. Hergert, and S. Doxsey. 2007. Loss of centrosome integrity induces p38-p53-p21-dependent G1-S arrest. *Nat. Cell Biol.* 9:160–170. http://dx.doi.org/10.1038/ncb1529

Nigg, E.A., and T. Stearns. 2011. The centrosome cycle: Centriole biogenesis, duplication and inherent asymmetries. *Nat. Cell Biol.* 13:1154–1160. http://dx.doi.org/10.1038/ncb2345

Ou, Y.Y., G.J. Mack, M. Zhang, and J.B. Rattner. 2002. CEP110 and ninein are located in a specific domain of the centrosome associated with centrosome maturation. *J. Cell Sci.* 115:1825–1835.

Pampliega, O., I. Orhon, B. Patel, S. Sridhar, A. Díaz-Carretero, I. Beau, P. Codogno, B.H. Satir, P. Satir, and A.M. Cuervo. 2013. Functional interaction between autophagy and ciliogenesis. *Nature*. 502:194–200. http://dx.doi.org/10.1038/nature12639

Schmidt, K.N., S. Kuhns, A. Neuner, B. Hub, H. Zentgraf, and G. Pereira. 2012. Cep164 mediates vesicular docking to the mother centriole during early steps of ciliogenesis. *J. Cell Biol.* 199:1083–1101. http://dx.doi.org/10.1083/jcb.201202126

Schmidt, T.I., J. Kleylein-Sohn, J. Westendorf, M. Le Clech, S.B. Lavoie, Y.D. Stierhof, and E.A. Nigg. 2009. Control of centriole length by CPAP and CP110. *Curr. Biol.* 19:1005–1011. http://dx.doi.org/10.1016/j.cub.2009.05.016

Seeley, E.S., and M.V. Nachury. 2010. The perennial organelle: assembly and disassembly of the primary cilium. *J. Cell Sci.* 123:511–518. http://dx.doi.org/10.1242/jcs.061093

Sorokin, S. 1962. Centrioles and the formation of rudimentary cilia by fibroblasts and smooth muscle cells. *J. Cell Biol.* 15:363–377. http://dx.doi.org/10.1083/jcb.15.2.363

Spektor, A., W.Y. Tsang, D. Khoo, and B.D. Dynlacht. 2007. Cep97 and CP110 suppress a cilia assembly program. *Cell*. 130:678–690. http://dx.doi.org/10.1016/j.cell.2007.06.027

Stinchcombe, J.C., and G.M. Griffiths. 2014. Communication, the centrosome and the immunological synapse. *Philos. Trans. R. Soc. Lond. B Biol. Sci.* 369:20130463. http://dx.doi.org/10.1098/rstb.2013.0463

Tang, C.J., R.H. Fu, K.S. Wu, W.B. Hsu, and T.K. Tang. 2009. CPAP is a cell-cycle regulated protein that controls centriole length. *Nat. Cell Biol.* 11:825–831. http://dx.doi.org/10.1038/ncb1889

Tang, Z., M.G. Lin, T.R. Stowe, S. Chen, M. Zhu, T. Stearns, B. Franco, and Q. Zhong. 2013. Autophagy promotes primary ciliogenesis by removing OFD1 from centriolar satellites. *Nature*. 502:254–257. http://dx.doi.org/10.1038/nature12606

Tanos, B.E., H.J. Yang, R. Soni, W.J. Wang, F.P. Macaluso, J.M. Asara, and M.F. Tsou. 2013. Centriole distal appendages promote membrane docking, leading to cilia initiation. *Genes Dev.* 27:163–168. http://dx.doi.org/10.1101/gad.207043.112

Tsang, W.Y., A. Spektor, D.J. Luciano, V.B. Indjeian, Z. Chen, J.L. Salisbury, I. Sánchez, and B.D. Dynlacht. 2006. CP110 cooperates with two calcium-binding proteins to regulate cytokinesis and genome stability. *Mol. Biol. Cell.* 17:3423–3434. http://dx.doi.org/10.1091/mbc.E06-04-0371

Tsang, W.Y., C. Bossard, H. Khanna, J. Peränen, A. Swaroop, V. Malhotra, and B.D. Dynlacht. 2008. CP110 suppresses primary cilia formation through its interaction with CEP290, a protein deficient in human ciliary disease. *Dev. Cell*. 15:187–197. http://dx.doi.org/10.1016/j.devcel.2008.07.004

Ying, G., P. Avasthi, M. Irwin, C.D. Gerstner, J.M. Frederick, M.T. Lucero, and W. Baehr. 2014. Centrin 2 is required for mouse olfactory ciliary trafficking and development of ependymal cilia planar polarity. *J. Neurosci.* 34:6377–6388. http://dx.doi.org/10.1523/JNEUROSCI.0067-14.2014